Bulletin of Earth Sciences of Thailand

RESERVOIR CHARACTERIZATION USING ROCK PHYSICS AND SPECTRAL DECOMPOSITION, PATTANI BASIN, GULF OF THAILAND

Sabrina Sultana Snigdha*

Petroleum Geoscience Program, Department of Geology, Faculty of science,
Chulalongkorn University, Bangkok 10330, Thailand
*Corresponding author email: du.snigdha@yahoo.com

Abstract

The aim of the present study is to apply rock physics for a better understanding of rock properties of various lithologies and apply spectral decomposition technique for the prediction of hydrocarbon zones in Pattani Basin of the Gulf of Thailand. Rock physics analysis reveals that seismic inversion techniques could not always differentiate lithologies and reservoir fluids due to similar rock physics properties of various lithologies. Reservoir wedge modeling, spectral decomposition of the synthetic and field data were conducted to understand the spectral decomposition response to thickness variation and reservoir fluids. Results revealed that gas saturated zones have high amplitudes as compared to water-wet zones, and the contrast is significant in the case of extremely low frequencies (from 10 to 15 Hz) outputs of far angle partial stacks. Organic shales show bright amplitudes on the seismic section, which are similar to the gas sands. However, spectral decomposition of synthetic seismogram of these shales indicates that it consists of only relatively higher frequencies (greater than 25Hz), and low frequencies are missing within the organic shales. Based on the results of synthetic modeling, it is inferred that gas sands can be differentiated by using low frequencies (10 to 15 Hz). Horizon slices, extracted from low-frequency volumes of the spectral decomposition of far angle partial stacks show the spatial distribution of hydrocarbons which match with existing well data. Hence, this workflow is useful for reservoir characterization where conventional seismic inversion techniques fail due to similar rock physics properties of different lithologies and fluids.

Keywords: Rock Physics Analysis, Reservoir wedge modeling, Spectral decomposition, Low frequency anomalies.

1. Introduction

The Pattani Basin of the Gulf Thailand is one of the major hydrocarbon producing areas of Thailand (Figure 1). The depositional sequences within the Pattani Basin consist of lacustrine, fluvial, (dominant) and marginal marine sediments. The reservoirs in the area are predominantly Lower to Middle Miocene fluvial channels and overbank sands. The reservoir sands show large lateral and vertical changes. Due to variable types of sediments and different depositional environments, it is difficult to predict subsurface lithologies and hydrocarbons based on post-stack seismic attributes and post-stack seismic inversion (Ahmad & Rowell, 2012 and Ahmad & Rowell, 2013). Therefore, it is required to understand the rock properties within the each stratigraphic sequence and to devise an effective workflow for hydrocarbon prediction. The present study applied rock physics to understand the rock properties of different depositional sequences and evaluated various parameters for the identification of lithologies and hydrocarbons. Spectral decomposition techniques have been useful for hydrocarbon reservoir characterization at various areas of the world (Castagna et al., 2003 and Chen et. al, 2008). Although there have been successful attempts to predict lithologies within the Pattani Basin by using spectral decomposition (Ahmad & Rowell, 2014), there is no case study reported for the application of spectral decomposition as a direct hydrocarbon indicator in the study area. In this research, I studied spectral decomposition response of different reservoir fluids and of organic-rich shales. Various models were analyzed to observe spectral decomposition response of fluids and thickness and optimum selected frequencies were applied for the prediction of hydrocarbons.

2. Methodology

2.1 Rock Physics Analysis

The well-log data for ten wells drilled in the

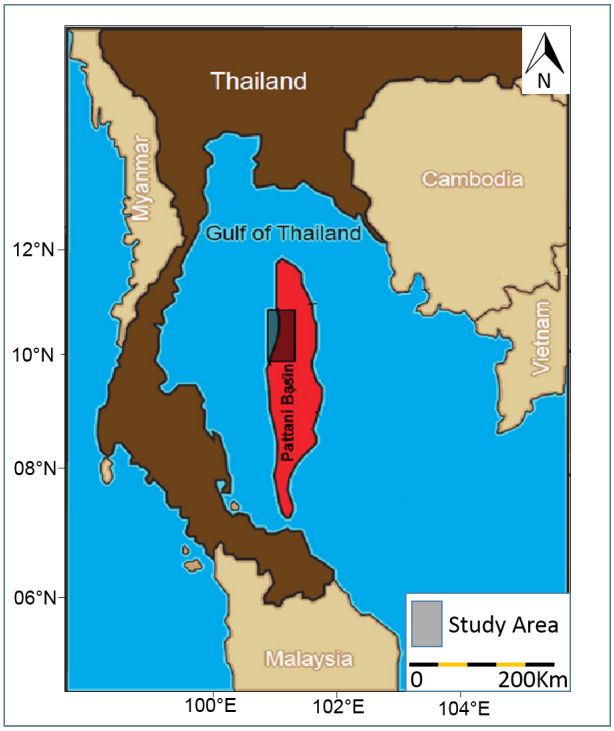

Figure 1. Study area located in the northern part of Pattani Basin, Gulf of Thailand.

study area were used for rock physics the reservoir zone. Several cross-plots were analyzed such as P-impedance, Vp/Vs and density with respect to petrophysical parameters such as shale volume and water saturation to find effective rock properties for lithology and fluid identification. The cut-off for water saturation is defined as 65% for the gas reservoir.

2.2 Spectral Decomposition

Spectral decomposition techniques typically generate a continuous volume of instantaneous spectral attributes from broadband seismic data, to provide useful information for reservoir characterization and direct hydrocarbon detection (Partyka et al., 1999; Castagna et al., 2003; Liu and Marfuit, 2007). Low-frequency energy anomalies associated with reservoirs have been observed for many years. Taner et al. (1979) noted the occurrence of low frequencies beneath gas and condensate reservoirs. Castagna et al. (2003) showed that low frequency shadows could identify gas reservoirs.

In the study area, the spectral decomposition method was used to extract the characteristic frequency components to determine the frequency anomalies associated with thin gas sands. Two types of systematic three-layer wedge models for thickness variation and fluid content at different stratigraphic sequences were created: a) low impedance gas sand is sandwiched between two high impedance shale and b) wet sand is encased in between shale. Rock properties of sand and shale in the models were taken from the original logs. Synthetic seismograms of these wedge models were generated using a plane wave convolution approach. Extracted wavelets within specific sequences were used for convolution.

These synthetic seismograms were spectrally decomposed from 10Hz up to 70Hz using Fast Fourier Transform (FFT) and Continuous Wavelet Transform (CWT) algorithm. In Fast Fourier Transform (FFT), a short temporal window (24 ms) within the zone of interest was transformed from the time domain into the frequency domain. The outputs of this process are frequencies slices generated over a time-windowed zone of interest. Continuous Wavelet Transform (CWT) compares a signal with shifted and scaled (stretched or shrunk) copies of a basic wavelet ("Mexican Hat" wavelet was used in this study). CWT uses inner products to measure the similarity between signals and provides a different approach to time-frequency analysis. The output of both FFT and CWT methods is time-frequency volume (Castagna, J. P. and Sun, S., 2006). However, CWT method provides fine details of the signal both in time and in frequency as it does not depend upon window length. The spectral amplitude of each frequency was analyzed for thickness variationand fluids. I selected appropriate spectral decomposition algorithm for the identification of more pronounced fluid effect. The studystarted by analyzing the influence of layer thickness on the frequency response, especially when the Because in this region, the reflected events from the top layer and the bottom layer overlap and produce a compound signal whose peak frequency depends on thickness. After layer thickness increases beyond one-half wavelength, the two events

can be separated in two-way travel time. To study the tuning thickness effect on the frequency by using wedge model, effective tuning thickness for ach frequency was computed by analyzing spectral amplitudes.

Near-, mid- and far- partial angle synthetic seismograms were computed and spectrally decomposed to identify the effect of fluids.

Based on synthetic seismogram results, optimum frequencies were selected for differentiation of gas sands.

3. Results and Discussions

3.1 Rock Physics Analysis

Figure 2(a) shows the cross plot of density versus shale volume colored by depth for the total stratigraphic section. It is observed that sands have lower density compared to shale within all depth intervals. In Sequence IV the contrast between sand and shale is higher and reduces as depth increases (Figure 2a). The relationship between P-wave velocity and shale volume, P-wave velocity decreases with increasing shale percentage. Similarly within Sequence III, P-wave velocity increases with the increase of shale percentage until 45 percent. Then gradually P-wave velocity shifts toward low values as shale percentage increases. P-wave velocity decreases very slightly as the shale percentage increases within Sequence II.

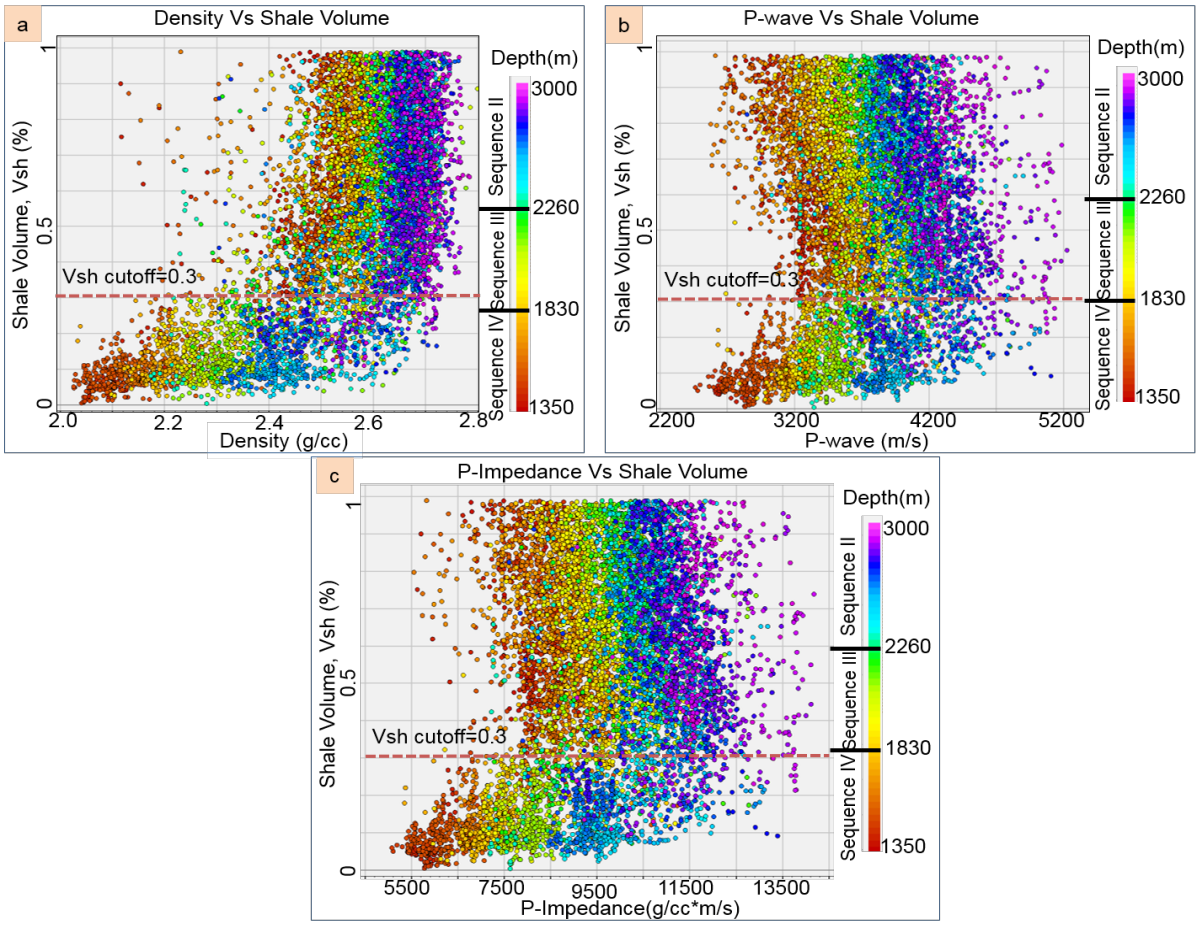

Figure 2. (a) Cross plot of density and shale volume of the total stratigraphic section. (b) Cross plot of P-wave velocity and shale volume of the total stratigraphic section. (c) Cross plot of P-impedance and shale volume of the total stratigraphic section.

The P-wave velocity of sand and shale overlap. The P-wave velocity of sand and shale overlap. P-impedance dependents on depth (Figure 2c). In the shallow section it is observed that sands have lower P-impedance than shales but in the deeper sections, sands and shales have less contrast in terms of P-impedance. P-impedance increases as shale percentage increases to 30% and beyond 30% there is a slight decrease in P-impedance.

Cross plot of density versus shale volume colored by water saturation in Sequence IV in two different wells which are 2km apart are shown in Figure 3(a) and Figure 3(b). For the both cases, sands can be separated from shales using density within the Sequence IV. In one of the wells, gas sands show different density from wet sands (Figure 3a), whereas the other well shows the same density for gas sands and wet sands (Figure 3b).

density than shales but gas saturated sands cannot

Similarly, P-impedance is also not consistent for gas sands. Gas sands do not show different P-impedance for all wells as compared to wet sands. In some wells, gas sands have distinctive P-impedance (Figure 4a) while in other wells P-impedance of gas sands and wet sands is the same (Figure 4b) for the shallow Sequence IV. However, P-impedance for sands and shales is different throughout the Sequence IV.

P-impedance versus Vp/Vs cross plot in Sequence IV of two wells illustrates that gas sands have low P-impedance and low Vp/Vs (Figure 4c and 4d) with partial overlapping of provide an accurate prediction of gas sands within Sequence IV. P-impedance versus Vp/Vs cross plot in Sequence IV of two wells illustrates that gas sands have low P-impedance be separated from water saturated sands based on density in Sequence III (Figure 5a and 5b). It

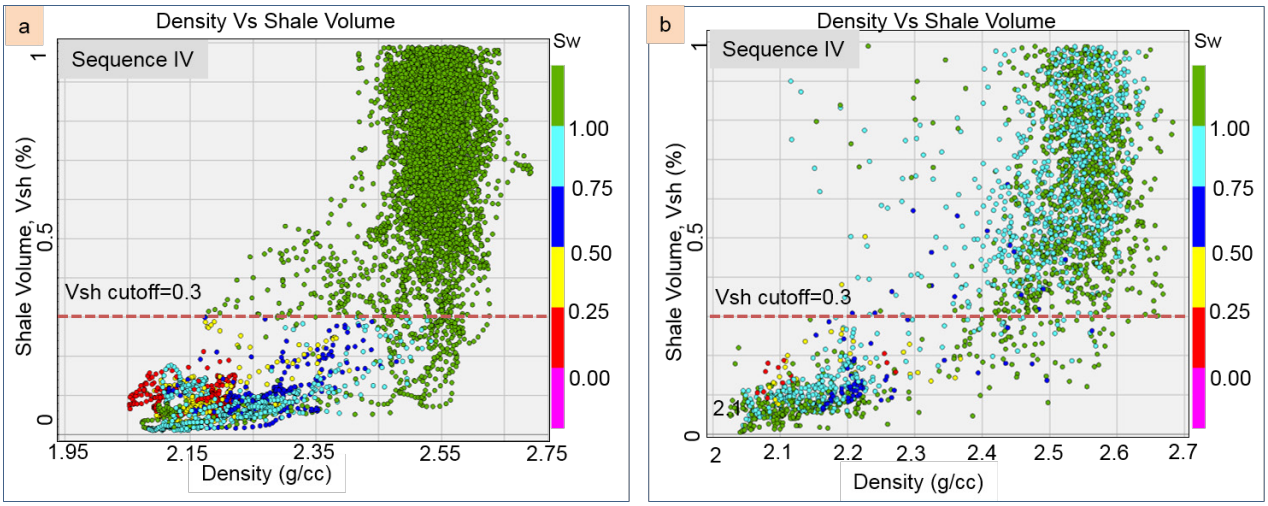

Figure 3. Cross plot of density and shale volume colored by water saturation within Sequence IV in two different wells. (a) Gas sands show lower density than wet sand. (b) Gas sands and wet sands show similar values.

and low Vp/Vs (Figure 4c and 4d) with partial overlapping of some non-reservoir lithologies. Therefore, a combination of P-impedance and Vp/Vs may provide an accurate prediction of gas sands within Sequence IV.

Figure 5(a) and 5(b) shows the cross plot of density versus shale volume colored by water saturation within Sequence III in two different wells. It is noticed that sands have lower

is observed that some shale points have a very low density (Figure 5b). In the well section, it is identified that these shale points with very low density also show very low P-velocity, low P-impedance, low Vp/Vs with a high gamma ray values (>200API) (Figure 5c). Ying Li at al. (2014) studied a rock physics model for the characterization of organic shale (Li Y, Guo ZQ, Liu C, et al., 2015). They explained that the

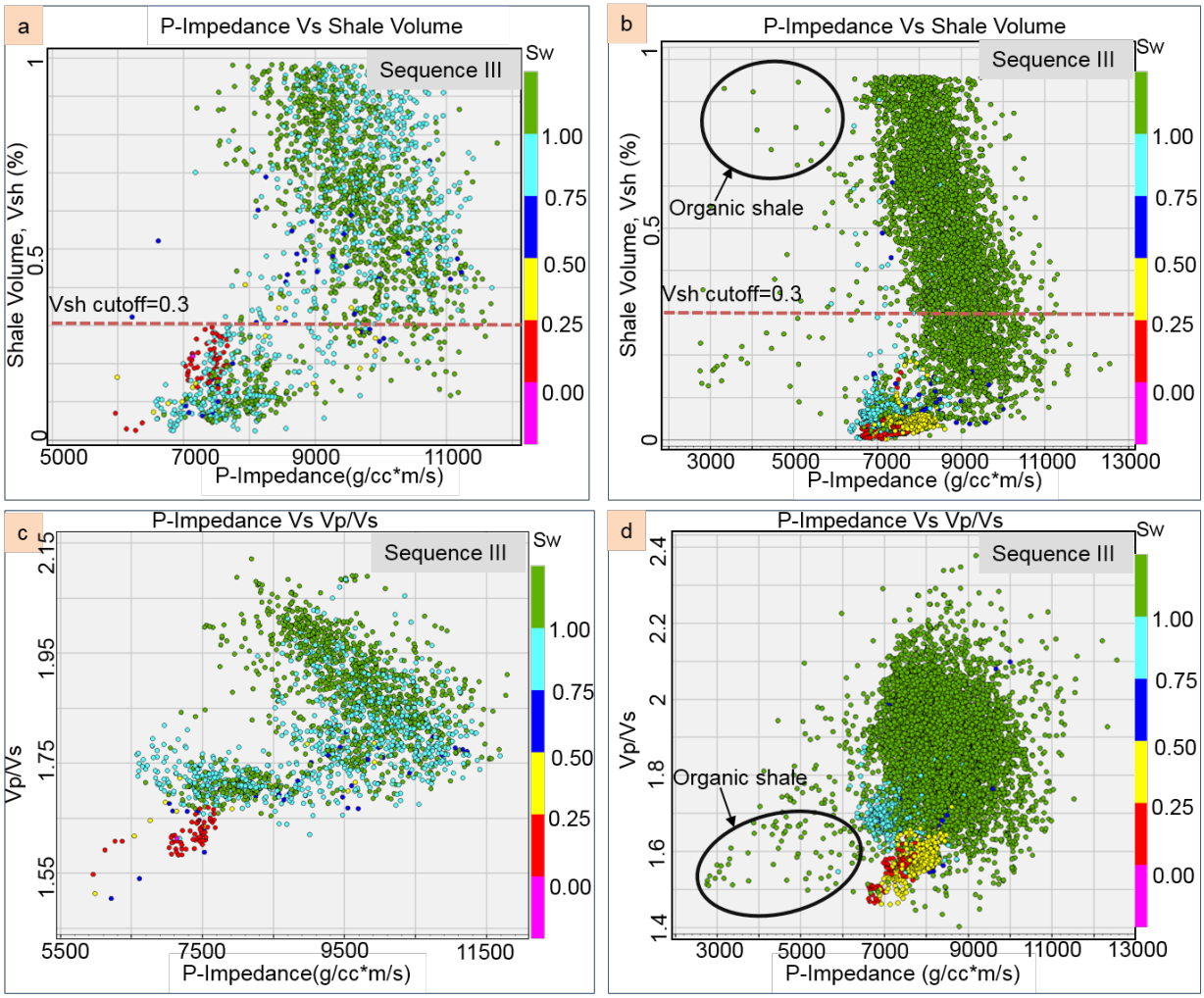

Figure 4. (a) Cross plot of P-impedance and shale volume in the well where gas sands can be separated from wet sand. (b) Cross plot of P-impedance and shale volume in the well location where gas sands cannot be separated from wet sand. (c) Cross plot of P-impedance and Vp/Vs in the well location where gas sands can be separated from wet sand. (d) Cross plot of P-impedance and Vp/Vs in the well location where gas sands cannot be separated.

increase of kerogen content and IV. These organic shales are not spatially homogeneously distributed within the Sequence III.

Cross-plots of P-impedance and shale volume indicates that P-impedance of sand is relatively low in the Sequence III (Figure 6a, 6b). P-impedance can clearly differentiate sand and shale in wells where there is limited presence of organic shales (Figure 6a), but P-impedance fails to separate sands and shales when organic shales are present (Figure 6b). P-impedance cannot discriminate pore fluids regardless whether organic shales are present or not (Figure 6a and 6b). Cross plot of P-impedance versus Vp/Vs reveals that gas sands have low P-impedance, and low Vp/Vs. The combination of these two parameters can separate gas saturated sands and water wet sands, where the presence of organic shale is limited (Figure 6c). Cross plot of P-impedance and Vp/Vs (Figure 6d) shows that organic shales have even lower P-impedance and Vp/Vs than gas sands. In the presence of organic shales, P -impedance and Vp/Vs combination is not effective to separate lithology and fluids within the Sequence III.

In Sequence II, density of sands and shales is different. Sands show low density as compared to shales (Figure 7a). P-impedance and shale volume cross plot (Figure 7b) in Sequence II indicates that P-impedance values

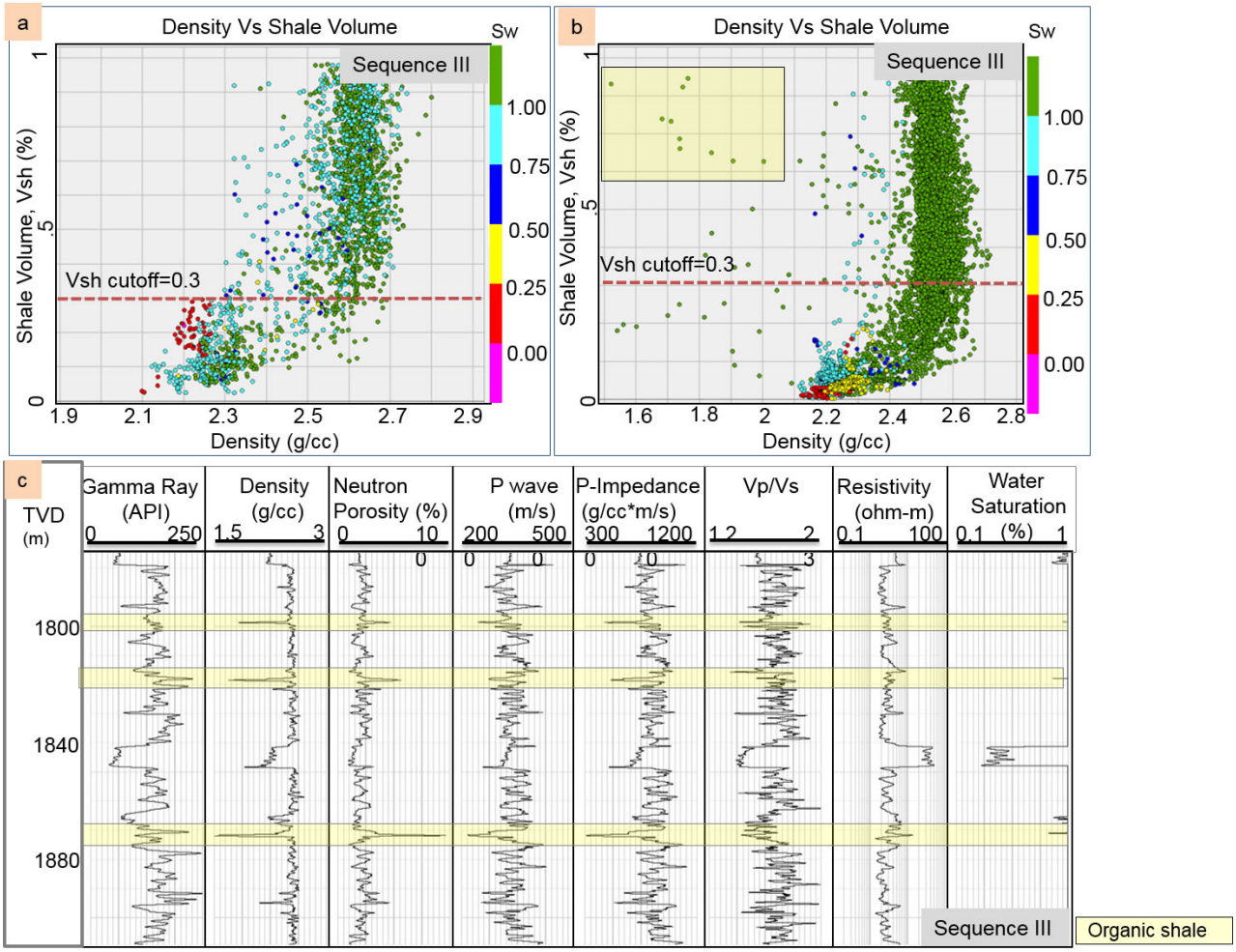

Figure 5. (a) Cross plot of P-impedance and shale volume in Sequence III where organic shales are absent.(b) Cross plot of P-impedance and shale volume where organic shales are present. (c) Vertical section showing gamma ray, density, neutron porosity, P-impedance, Vp/Vs, resistivity and water saturation response within Sequence III.

Only clean sands (less than 10% shale volume) can be isolated based on P-impedance. Gas sands cannot be discriminated based on P-impedance. P-impedance versus Vp/Vs cross plot colored by water saturation in Sequence II (Figure 7c, Figure 7d) shows that gas sands have low P-impedance and Vp/Vs but there are some points of organic shales which are in the same range. Gas sands can be partially separated by using P-impedance and Vp/Vs within the Sequence II. It is observed that in the well section where there is lack of organic shale, a combination of P-impedance and Vp/Vs can be used to identify gas sands. However, the presence of organic shales makes P-impedance and Vp/Vs combination less effective for the prediction of the hydrocarbon zones.

3.2 Spectral Decomposition

Figure 8(a) shows zero offset synthetic seismogram of Sequence III from wedge model of gas saturated sand sandwiched between two high impedance symmetric shales. The P-impedance of gas sand, wet sand and shale used in this model are 7107.25 (m/s)*(g/cc), 8697.46 (m/s)*(g/cc) and 12348.7 (m/s)*(g/cc) respectively. Extracted wavelet from Sequence III with a peak frequency of 30Hz was convolved with the model to generate synthetic traces.

The relationship between peak energy versus gross reservoir thickness indicates maximum peak energy occurs at 17m (Figure 8b). This highest energy is due to tuning thickness because of constructive interference of reflections for gas saturated sand. Similarly, tuning

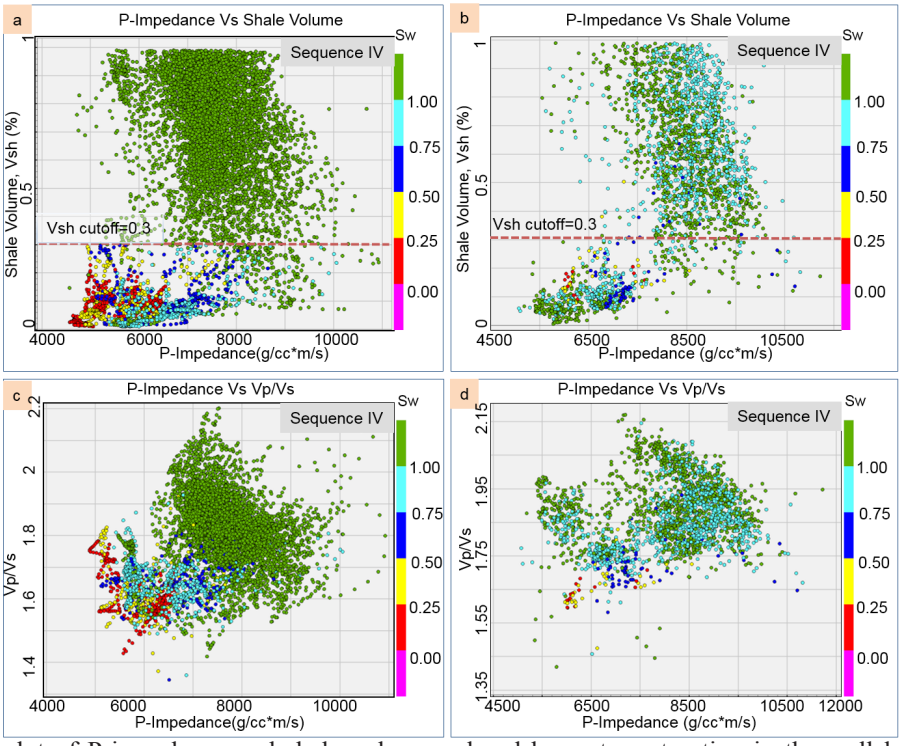

Figure 6. (a) Cross plot of P-impedance and shale volume colored by water saturation in the well location where organic shale is absent within Sequence III.(b) Cross plot of P-impedance and shale volume where organic shale is present within Sequence III. (c) Cross plot of P-impedance and Vp/Vs in the well location where organic shale is absent within Sequence III.(d) Cross plot of P-impedance and Vp/Vs in the well location where organic shale is present within Sequence III

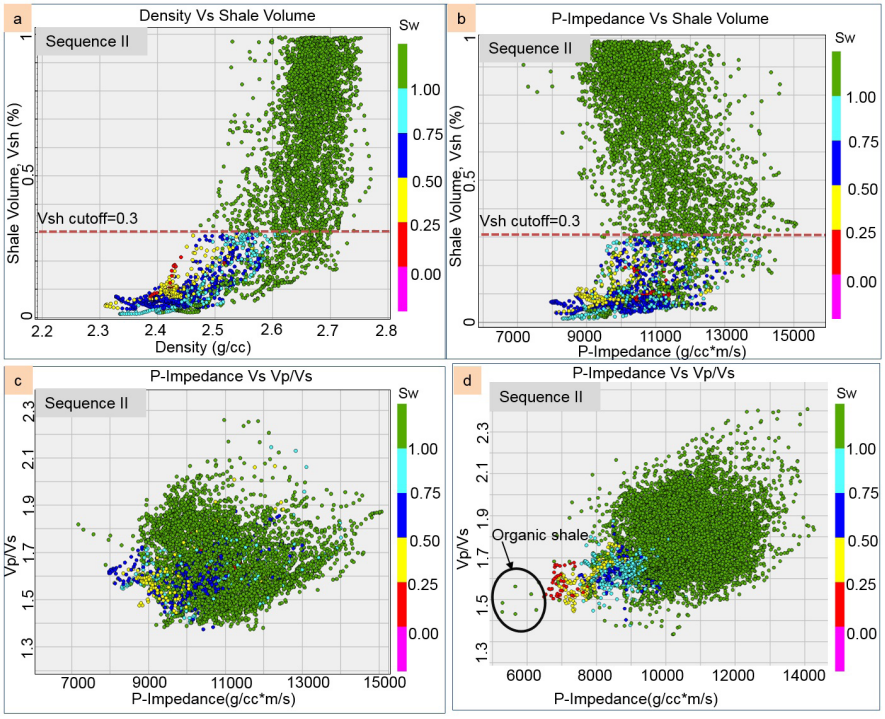

Figure 7. (a) Cross plot of density and shale volume within Sequence II. (b) Cross plot of P-impedance and shale volume within Sequence II.(c) Cross plot of P-impedance and Vp/Vs within Sequence II. (d) Cross plot of P-impedance and Vp/Vs in the well location where organic shales are present within Sequence II.

thickness of wet sand is 20m.

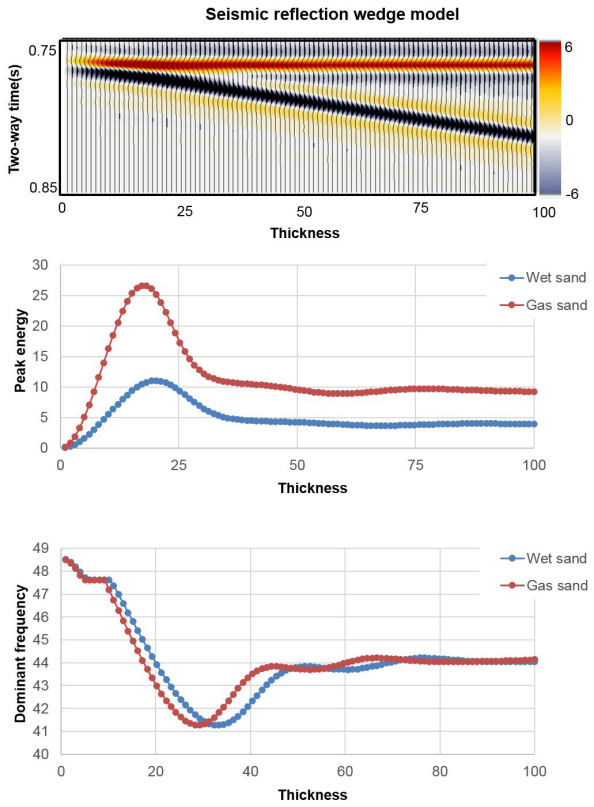

Figure 8. (a) Synthetic seismic traces of the wedge model of gas saturated sand encased in symmetric shales. (b) Peak energy versus gross reservoir thickness of full stack equivalent seismogram of gas and wet sand model (c) Dominant frequency versus gross reservoir thickness of full stack equivalent seismogram of gas and wet sand model.

Figure 8(b) shows that gas sands have a higher amplitude as compared to wet sands. Amplitude depends on gas as well as thickness. It is observed that maximum energy occurs at tuning thickness. The water-filled reservoir at tuning thickness (at λ/4=20m) yields similar amplitude as of gas sands at a greater thickness (at λ/2 =34m). As a result, high amplitude on full stack seismic data may be due to the presence of gas sands or due to tuning the effect of water wet sands. Therefore, high amplitude anomalies associated with tuning thickness of wet sands can be misleading.

Figure 8(c) illustrates peak frequency versus gross reservoir thickness from hydrocarbon models and the wet sand models. Peak frequencies decrease monotonically with increasing gross reservoir thickness up to 30m for both gas and wet sand model.

Spectral decomposition analysis of different algorithms such as Fast Fourier Transform (FFT) and Continuous Wavelet Transform (CWT) are shown in Figure 9 and 10. Amplitude spectra of FFT (Figure 9) at different frequencies for wet sands at tuning thickness (λ/4 =20m) is similar to gas saturated sands at half of wavelength (λ/2 =34m). Whereas, amplitude spectra of CWT (Figure 10) shows a different pattern for gas sands and wet sands. Gas sands at half of wavelength (λ/2 =34m) show high amplitudes at low frequency as compared to wet sands at tuning thickness of (λ/4=20m). Hence amplitude anomalies obtained by CWT algorithm at low frequencies may be helpful to separate anomalies due to gas sands and tuning effect of wet sands.

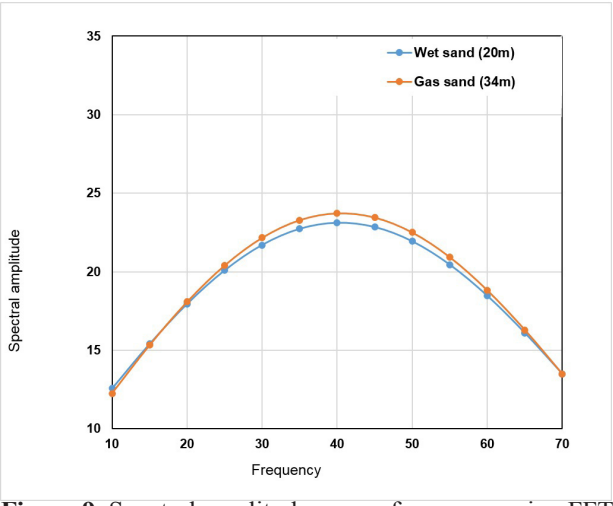

Figure 9. Spectral amplitude versus frequency using FFT algorithm for the wet sand model having 20m thickness (at tuning thickness) and gas model having 34m thickness.

The tuning thickness of gas saturated sands at specific iso-frequency section is identified using thickness versus spectral amplitude graph shown in Figure 11. For example, at 35Hz the highest spectral amplitude occur at 17m. It indicates that tuning thickness is of 17m for 35Hz frequency. Figure 11 demonstrates that at high frequencies maximum amplitude shifts to lower thickness. For example at 65Hz, 50Hz,

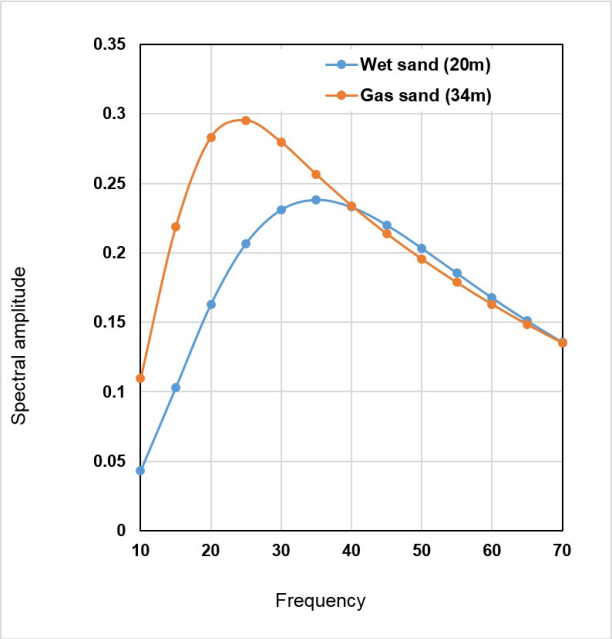

Figure 10. Spectral amplitude versus frequency using CWT algorithm for the wet sand model having 20m thickness (at tuning thickness) and gas model having 34m thickness.

35Hz, 20Hz iso-frequencies, tuning thickness occur at 14m, 15m, 17m and 28m layer thickness respectively.

To identify fluid effect, four models of zero offset, near (5^0 -22^0), mid (20^0-35^0), far (35^0 -55^0) angle partial stacks were created and compared. The thickness of gas sands in these models are equal to half of wavelength (34m) and encased in between shales. The greater thickness was selected to avoid interference effects. Amplitude spectra of gas sands is high for all frequencies as compared to wet sands (Figure 12). Amplitude spectra of gas sands are broad, and it consists of amplitudes at lower frequencies as well as at higher frequencies. The low-frequency component is prominent in all the cases (Zero offset, near, mid and far angle partial stacks) for the gas sands. The low-frequency amplitudes are relatively weak in wet sands (Figure 12 a, b, c, d). This effect is mostly significant in lower frequencies for the case of far angle partial stack. For example in

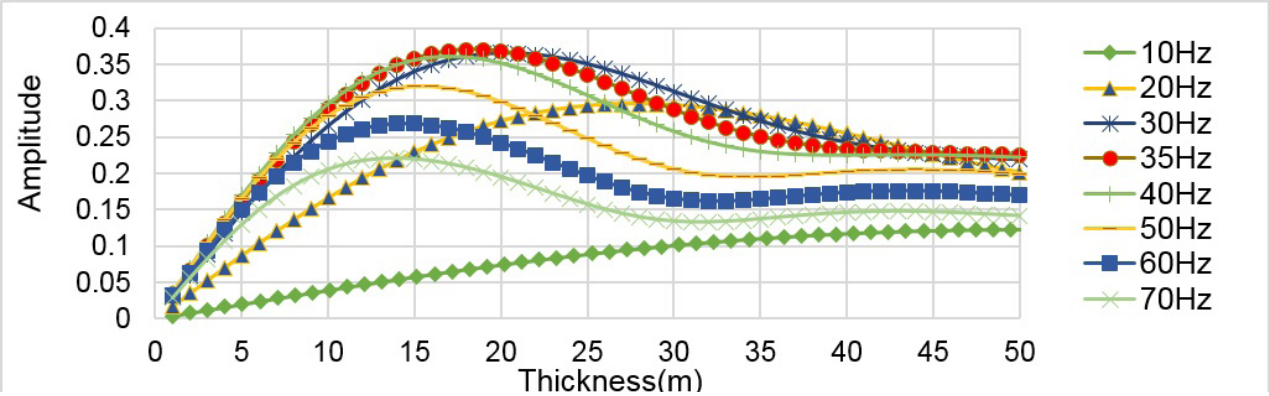

Figure 11. Spectral amplitude versus thickness of gas saturated sands model in Sequence III.

the case of zero offset, at 18Hz, the amplitudes of gas sands are bright, but wet sands at 18Hz show very low values of amplitudes (Figure 12a). In the case of the far angle partial stack, high amplitudes can be observed for gas sands at 12Hz, whereas in regard to wet sands, amplitudes at 12 Hz are dim (Figure 12d)

Rock physics analysis revealed that P-impedance of organic-rich shales is less than gas sands. Therefore, these shales produce bright amplitude on the seismic seismogram (Figure 13). These high amplitudes can be mistakenly considered as sands or gas bearing sands. It is not possible to differentiate bright amplitudes associated with organic shales and gas sands on full stacks seismic data.

Time-frequency section for the zone comprising thin organic shales indicates that high amplitudes are distributed in the high-frequency zone, and organic shales do not show amplitudes for low frequency (Figure 14a). Whereas, gas sands shows very high amplitudes

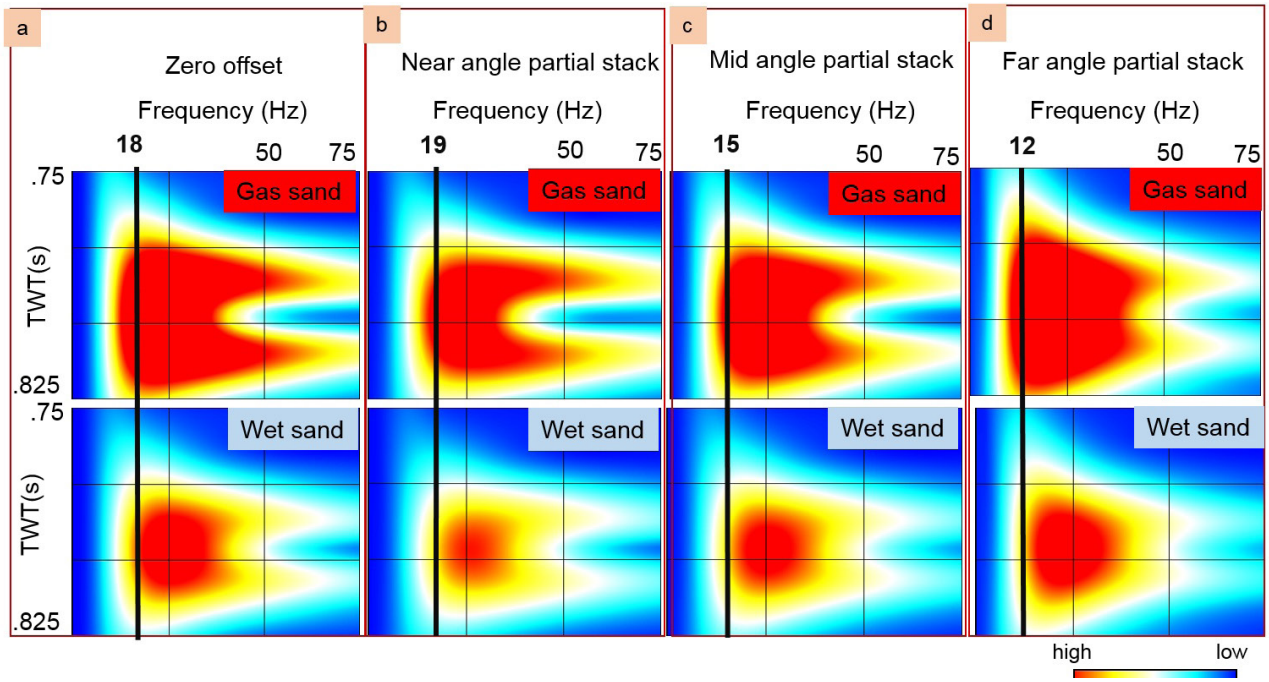

Figure 12. Spectral decomposition response of gas and wet sand on (a) Zero offset, (b) near angle partial stack, (c) mid angle partial stack and (d) far angle partial stack synthetic seismograms

at lower frequencies for both zero offset (Figure 14b) and far angle modeled synthetics (Figure 14c).

As demonstrated by Figure 12, gas effect is more pronounced in the case of far angle partial stacks. Hence spectral decomposition could successfully differentiate organic shales and gas sands in the low-frequency spectra of far angle partial stack.

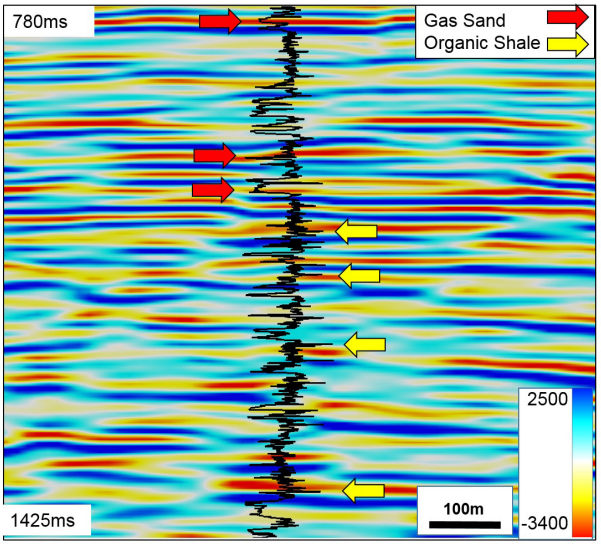

Figure 13. Seismic section within Sequence III along the well showing GR. Yellow arrows mark the bright spots associated with the organic shales

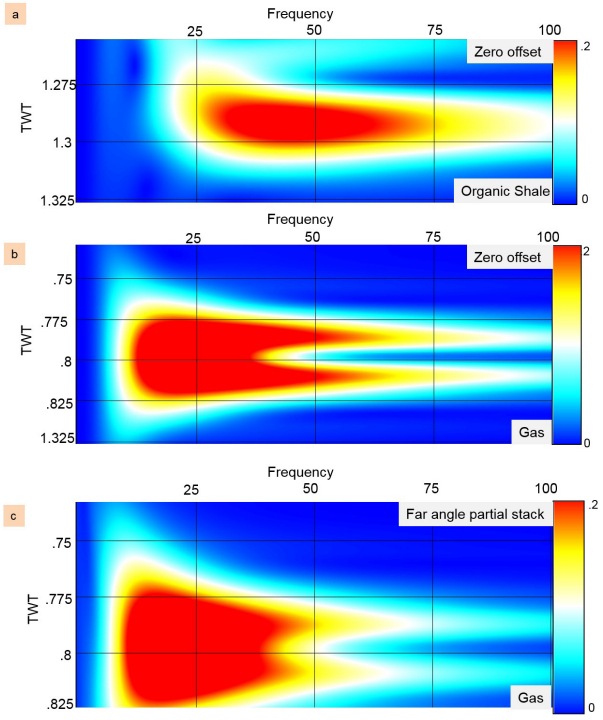

Figure 14. (a) Spectral decomposition response of organic shales b) Spectral decomposition response of gas sands at zero offset. (c)Spectral decomposition response of gas sands at far angle partial stack.

The horizon slice within Sequence III (Figure 15) extracted from 12 Hz frequency volumes of the spectral decomposition of far angle partial stacks

shows the spatial distribution of hydrocarbons. It is observed that within Sequence III, sands can be imaged by the values in between 90 to 120 (Figure 15). Moreover, most of the values higher than 130 represent gas sands within Sequence III. The large red-yellow body in Figure 15(a) represents the clear trend of gas sand distribution, and the circles represent the proved results of wells from well data. There are 5 wells which penetrated at the red zones found the hydrocarbon sands whereas the other 5 wells, which penetrated the blue zones found wet sands. Therefore, low-frequency spectral decomposition horizon slices provide useful information about reservoir distribution to reduce the exploration and development risks.

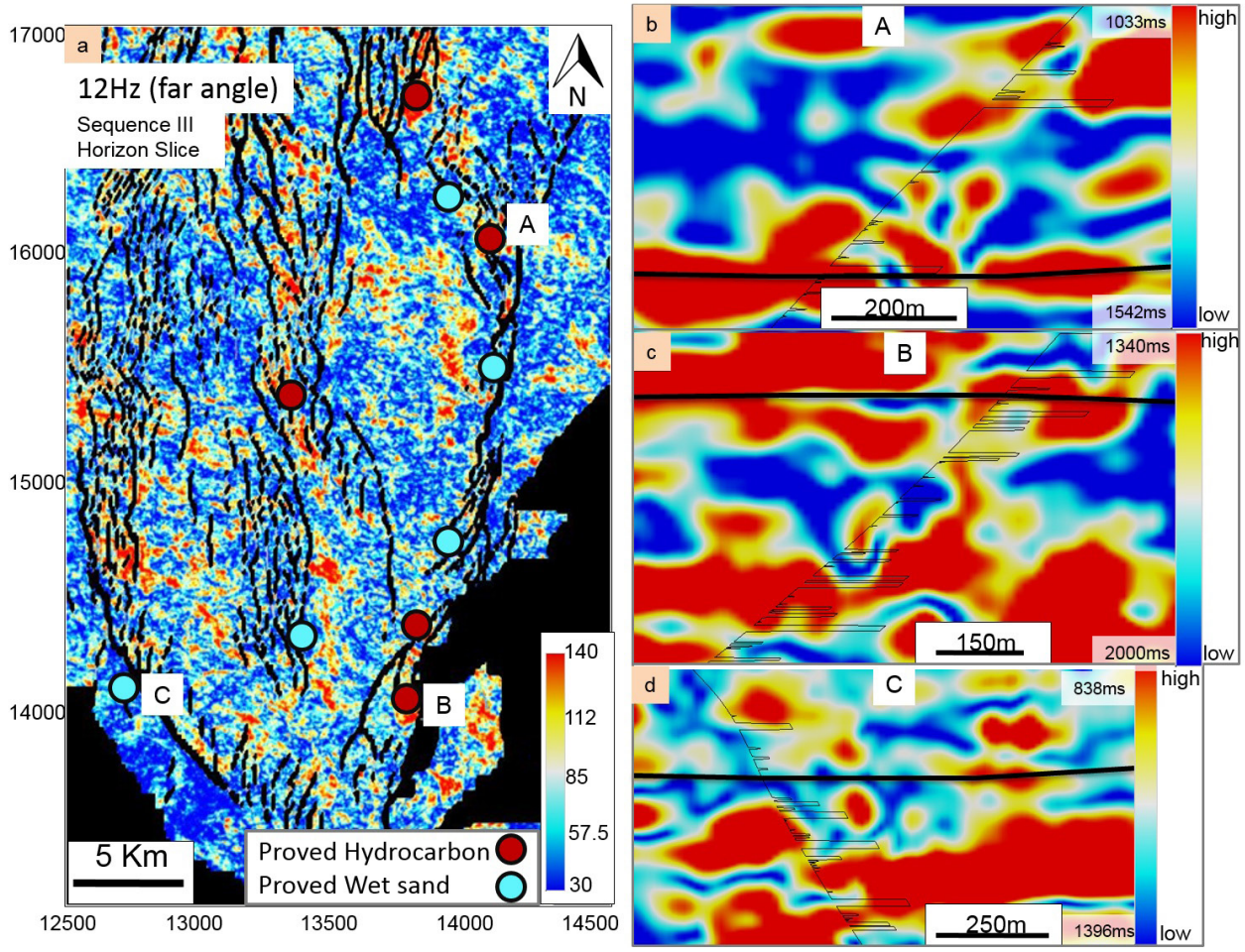

Figure15. (a) Amplitude spectra of CWT at 12Hz (far angle partial stack) along the horizon slice within Sequence III. The bright amplitudes shows gas sand distributions.The bright anomalies associated with gas sand are confirmed by the net pay log in three different locations are shown on the vertical section in Figure (b), (c), (d).

4. CONCLUSIONS

The study area has heterogeneously distributed organic shales. These are mostly occur in the Sequence III, but occasionally also found in Sequence II and IV. The rock properties of these shales are similar to gas bearing sands, which makes difficult to distinguish these shales and gas sands for most of the conventional seismic quantification techniques. Post-stack seismic inversion may not always capable of predicting the subsurface lithologies of the area especially within the Sequence III, where organic shales are abundant. The organic shales have low P-impedance, which is in the range of P-impedance of sands. Hydrocarbon zones cannot be differentiated by using inverted P-impedance volumes as gas saturated sands and wet sands have overlapping P-impedance.

However, the combination of Vp/Vs and P-impedance is capable of isolating hydrocarbon zones only in the shallow Sequence IV and could not isolate gas sands in other sequences of the zone of interest. Some of the organic-rich shales within the Sequence III exhibit low values of Vp/Vs and P-impedance, which is in the range of values of gas sands. AVO analysis may not work in areas where organic shales overlie the gas sands due to lack of contrast of Vp/Vs. Elastic impedance values for near (15°) and mid angle (30°) are simillar for gas sands and organic rich shales. Therefore, elastic impedance inversion may not be always useful for the detection of gas sands in Sequence III in the presence of organic shales. Model-based studies revealed that spectral decomposition using CWT algorithm gives better results as compared to FFT for the identification of gas sands. According to spectral decomposition analysis, local fluids and reservoir thickness are first-order factors to control spectral decomposition response in the study area. Amplitude contrast between gas and wet sands is significant in the case of low frequencies (10~15 Hz) and this contrast is more pronounced in far angle partial stacks. Amplitude anomalies at low frequencies outputs of spectral decomposition can isolate gas saturated zones and organic shales, because organic shales do not show high amplitudes at low frequencies. The separation of these organic shales were not otherwise possible through inversion and AVO techniques due to similar rock properties. Low-frequency anomalies (at 12 Hz) of spectral decomposition outputs of far angle partial stacks matched with the hydrocarbon distribution at the well locations. CWT algorithm of spectral decomposition may help to predict gas saturated zones in the Pattani Basin, which has similar rock properties for different lithologies.

5. REFERENCES

Ahmad, M. N. and Rowell, P., 2013, Mapping of fluvial sand systems using rock physics analysis and simultaneous inversion for density: case study from Gulf of Thailand: First break, v. 31, May 2013, p. 49-54.

Castagna, J. P. and Sun, S., 2006, Comparison of spectral decomposition methods, First Break, 24, p. 75-79.

Castagna, J. P., S. Sun, and R. W. Siegfried, 2003, Instantaneous spectral analysis: Detection of low-frequency shadows associated with hydrocarbons: The Leading Edge, 22, p. 120–127.

Chen G., G. Matteucci, B. Fahmy, C. Finn, Spectral-decomposition response to reservoir fluids from a deepwater West Africa reservoir, 2008, Geophysics ,Vol. 73, NO. 6, p. C23–C30

Deng, J., D. Han, J. Liu, Q. Yao., 2007, Application of Spectral Decomposition to Detect Deepwater Gas Reservoir, SEG Annual Meeting, p. 1427-1430.

Li Y, Guo ZQ, Liu C,et al.,2015, A rock physics model for the characterization of organic-rich shale from elastic properties, Petroleum Science,v.12,issue 2, p.264-272.

Tai S., C. Puryear, J. P. Castagna, 2009, Local frequency as a direct hydrocarbon indicator: SEG Annual Meeting, p. 2160-2163.